Journal of Power Sources 217 (2012) 175–183

Contents lists available at SciVerse ScienceDirect

Journal of Power Sources

journal homepage: www.elsevier.com/locate/jpowsour

Chemical aging of the silicone rubber in a simulated and three accelerated proton exchange membrane fuel cell environments

Guo Li, Jinzhu Tan, Jianming Gong*

School of Mechanical and Power Engineering, Nanjing University of Technology, Nanjing, Jiangsu 210009, China

HIGHLIGHTS

- The surface became rough and finally cracked for silicone rubbers after exposure.
- Chemical degradation is due to the chain scissoring in the backbone.
- The concentration of acid solution could accelerate the degradation of samples.
- Aging mechanisms are same for the samples exposed to different environments.

ARTICLE INFO

Article history:
Received 28 March 2012
Received in revised form
24 May 2012
Accepted 25 May 2012
Available online 6 June 2012

Keywords:
Aging
Silicone rubber
PEM fuel cell
ATR-FTIR
X-ray photoelectron spectroscopy

ABSTRACT

Long-term stability and durability of gaskets in Proton Exchange Membrane (PEM) fuel cell are important to both sealing and the electrochemical performance of PEM fuel cells. In this paper, the time-dependent aging process of silicone rubber, which is one of the potential gasket materials for PEM fuel cells, is investigated in one simulated PEM fuel cell environment and three accelerated durability test (ADT) media at 70 °C. Optical microscopy is employed to observe the topographical changes on the surfaces of samples. Attenuated total reflection Fourier transform infrared (ATR-FTIR) spectroscopy and X-ray photoelectron spectroscopy (XPS) are used to study the surface chemistry of the samples before and after exposure to the test environments over time. The optical microscopy results indicate that the surface conditions of the samples change from initially smooth to rough, crack appearance and finally crack propagation. The ATR-FTIR and XPS results reveal that the degradation mechanisms of the silicone rubber are likely due to the de-crosslinking and chain scission in the backbone, and the acid has a significant effect on the degradation.

© 2012 Elsevier B.V. All rights reserved.

1. Introduction

In order to keep the reactant gases (hydrogen and oxygen/air) within their respective regions, gaskets are required in Proton Exchange Membrane (PEM) fuel cells. The elastomeric gaskets used as seals in PEM fuel cells are exposed to acidic environment, humid air and hydrogen, and subjected to mechanical compressive pressure, their long-term stability and durability are critical to the performance of fuel cell. If any gasket degrades and loses its elastic property and seal functionality, the reactant gases may leak or mix each other directly during operation. This not only decreases the performance of fuel cell, but also poses a safety concern [1]. Therefore, the degradation of the elastomeric gaskets in PEM fuel cell environment over time is an important issue for PEM fuel cells. The thermal cycle, electrochemistry, or liquid/solid water may cause troubles to seals. The present study mainly focuses on the degradation of elastomeric gasket material used as seals in acidic environments for PEM fuel cell applications.

Many literature [2–4] reported the degradation of polymeric materials in irradiation environments. For instance, Akiyama et al. [2] studied the degradation process of Nafion by gamma-ray irradiation and heat treatment. Liu et al. [3] studied the degradation of DGEBA/DICY under 100 keV proton irradiation. Youn and Huh [4] investigated the surface degradation of silicone rubber and EPDM under accelerated ultraviolet weathering conditions. Some researchers [5–13] focused on the thermal degradation or aging process of elastomers exposed to different solutions. For example, Le Gac et al. [5] studied the aging mechanism and mechanical degradation behavior of polychloroprene rubber in a marine environment. Graiver et al. [6] reported a review on the effects and degradation process of silicones in outdoor environments. Mitra et al. [7–9] examined the chemical degradation of cross-linked fluoroelastomer in an alkaline environment and that of EPDM

* Corresponding author. Tel.: +86 13770923030; fax: +86 2558139361.
E-mail address: gongjm@njut.edu.cn (J. Gong).

0378-7753/$ – see front matter © 2012 Elsevier B.V. All rights reserved.
http://dx.doi.org/10.1016/j.jpowsour.2012.05.105

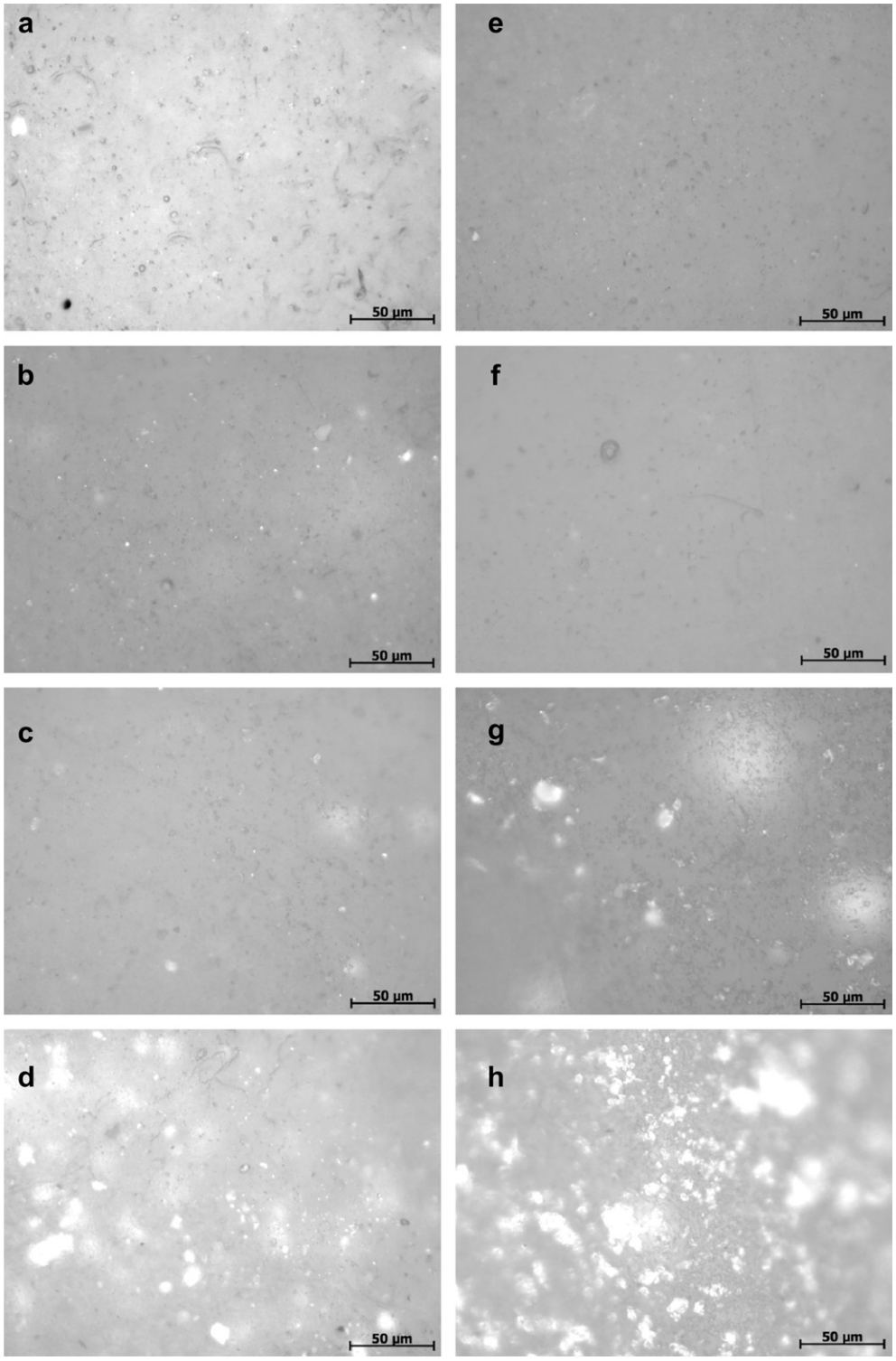

Fig. 1. Surface micrographs from the samples in test solutions: (a) before exposure, (b) after 432 h, (c) after 1992 h, (d) after 3312 h, (e) before exposure, (f) after 432 h, (g) after 1992 h, (h) after 3312 h, (i) before exposure, (j) after 432 h, (k) after 1992 h, (l) after 3312 h, (m) before exposure, (n) after 432 h, (o) after 1992 h, (p) after 3312 h.

rubber in a 20% Cr/H_2SO_4 acidic environment, respectively. Miwa et al. [10] studied the surface degradation of poly(ethylene-co-propylene-co-5-ethylidene-2-norbornene) terpolymer by ozone in water. Ghassemzadeh et al. [11] evaluated the chemical degradation of proton conduction perfluorosulfonic acid ionomers in a Fenton test by solid state 19F NMR spectroscopy. Hsu et al. [12] observed the moisture-related degradation of EPDM by electrical and SEM methods. Wang et al. [13] detected the aging behavior and thermal degradation of fluoroelastomer reactive blends with polyphenol hydroxy EPDM. Nowadays, there are more people concerning the degradation of materials in a simulated PEM fuel cell environment. Chen et al. [14] studied a synchronous investigation of the degradation of metallic bipolar plates in real and simulated environments of polymer electrolyte membrane fuel cells. Lin et al.

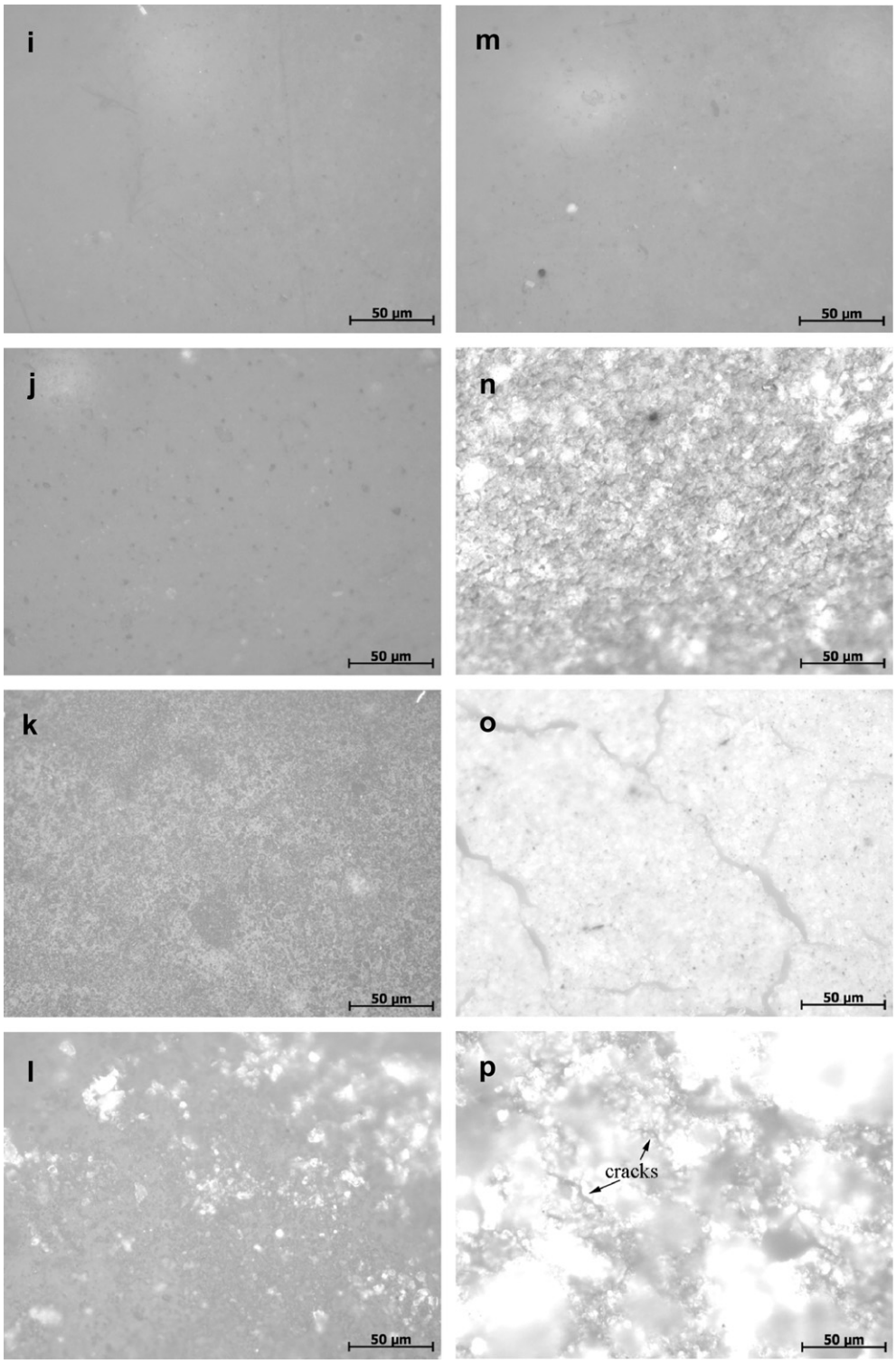

Fig. 1. (*continued*).

[15] investigated the chemical degradation of copolymeric resin, liquid silicone rubber, fluorosilicone rubber, EPDM and fluoroelastomer copolymer in a simulated and an accelerated PEM fuel cell environment at 80 °C. Tan et al. [16–20] studied the chemical and mechanical degradation of silicone rubber, fluoroelastomer and EPDM materials exposed to a simulated PEM fuel cell environment and one accelerated durability test solution at the temperatures of 60 °C and 80 °C. Wang et al. [21] reviewed the applications and current status of PEM fuel cell and the role of fundamental research. Borup et al. [22] had a review on scientific aspects of PEM fuel cell durability and degradation, including durability targets of USA, Japan and Europe, operational conditions effect on fuel cell durability, degradation of fuel cell components and so on.

In this paper, the aging process of the silicone rubber was studied in one simulated PEM fuel cell environment and three accelerated durability test solutions which were different from the

ones in our previous work [23]. High resolution analysis of X-ray photoelectron spectroscopy (XPS) was conducted in this study. The aim is (a) to investigate the degree of chemical degradation and degradation mechanisms for the silicone rubber samples exposed to four different acidic test solutions at the temperature of 70 °C for PEM fuel cells, and (b) to understand the effect of acid on the degradation for the PEM fuel cells. One regular solution (RS), similar to the real PEM fuel cell environment which has the PH value ranged from 3 to 4 [15,16] and three accelerated durability test (ADT) solutions were used. The ADT solutions were used for short-term, accelerated aging tests on the silicone rubber. The topographical changes on the surfaces of samples were detected using optical microscopy. The chemistry changes of the silicone rubber before and after exposure over time were studied by Attenuated total reflection Fourier transform infrared (ATR-FTIR) spectroscopy and X-ray photoelectron spectroscopy (XPS).

2. Experiments

2.1. Material and test environments

The silicone rubber studied in the work is a commercial elastomeric material. The rubber is a two-part formulation liquid injection molded material. It mainly contains polydimethylsilicoxane with vinyl functionalities in part A and polydimethylsilicoxane with hydrosilylation functionalities in part B. The part A and part B (1:1) combined and heated to crosslink under the platinum catalyzed reaction. The crosslinking mechanism is hydrosilylation. The fillers inside the material mainly include silica, quartz and calcium carbonate, etc.

Four solutions were used to age the material. The first solution is termed the "Regular" solution (RS), which is similar to the real PEM fuel cell environment. 48% hydrofluoric acid (HF) and 98% sulfuric acid (H_2SO_4) were dissolved in balance reagent grade water to make the test solutions. The composition of the regular solution is 12.5 ppm H_2SO_4, 1.8 ppm HF and reagent grade water having 18 Mega Ohm (MΩ) resistance. The regular solution has the PH value about 3.4.

Three ADT solutions, namely, ADT1, ADT2 and ADT3 solution, were used for short-term accelerated aging tests. Again, 48% HF and 98% H_2SO_4 were dissolved in balance reagent grade water to make the ADT solutions. The composition of ADT1 solution is 12.5 ppm H_2SO_4, 10 ppm HF and reagent grade water having 18 MΩ resistance. The composition of ADT2 solution is 12.5 ppm H_2SO_4, 50 ppm HF and reagent grade water having 18 MΩ resistance. The composition of ADT3 solution is 1 M H_2SO_4, 1.8 ppm HF and reagent grade water having 18 MΩ resistance.

The test temperature was selected at 70 °C which was close to the operating temperature of actual PEM fuel cells.

2.2. Aging and characterization methods

Rectangular-shaped samples with dimensions of 10 mm in length, 10 mm in width and 6 mm in thickness were prepared. Every two samples were put into one bottle with one solution. Four bottles containing four different solutions were then put into an oven with temperature of 70 °C. The aged samples were taken out and tested at selected times. The samples were cleaned using reagent grade water having 18 MΩ resistance to remove the excess acids and made dry at room temperature before the analysis.

The surface topographical changes were observed by optical microscope at selected times. ATR-FTIR spectroscopy was employed to investigate the surface chemistry of samples before and after exposure to the test environments using a Nexus Model 670 Instrument (Nicolet Instrument Corporation) which runs with 32 scans at a resolution of 0.1 cm^{-1}. The infrared radiation (IR) penetrates the surfaces of samples to approximately 1 μm.

XPS is quantitative, surface-sensitive and is able to distinguish different chemical states [24]. XPS analysis was performed using a Thermo Fisherscientific K-Alpha spectrometer with monochromatic Al Kα X-ray source. The survey spectra in the range of 0–1350 eV were recorded in 1 eV step for each sample. Atomic concentrations of each element were carried out by determining the relevant integral peak intensities. High-resolution analysis was conducted in the oxygen 1s (O1s) and the silicon 2p (Si2p) regions. The spectra were deconvoluted by curve-fitting. The high-resolution spectra were recorded in 0.1 eV step from which the detailed compositions were calculated.

3. Results and discussion

3.1. Microscopy

The topographical changes on the surfaces of samples before and after 3312 h exposure to the test solutions at 70 °C were obtained by optical microscopy as shown in Fig. 1. The magnification is 500×. The photos (a)–(d) in Fig. 1 indicate the surface micrographs of the samples exposed to the regular solution. The photos (e)–(h), (i)–(l) and (m)–(p) represent the surface micrographs of the samples exposed to ADT1 solution, ADT2 solution and ADT3 solution, respectively.

Fig. 1(a)–(d) represents the surface micro-topography changes of the silicone rubber before and after exposure to regular solution for 432 h, 1992 h and 3312 h, respectively. It can be found that the surface condition of the samples exposed to regular solution changed a little and no cracks appeared. The white spots (see Fig. 1(d)) were caused by degradation. And these white spots grew with the increase of aging hours (see Fig. 1(g), (h)) and increase of acid concentration (see Fig. 1(h), (p)). This result denotes that the degradation was not obvious for the samples after exposure to regular solution up to 3312 h.

Optical micrographs (e)–(h) in Fig. 1 indicate the surface micro morphology changes of the samples before and after exposure to ADT1 solution for 432 h, 1992 h and 3312 h, respectively. It can be seen that the surface of the sample became rough gradually with the exposure time.

The photos (i)–(l) in Fig. 1 show the typical surface condition of the silicone rubber before and after exposure to ADT2 solution for 432 h, 1992 h and 3312 h, respectively. The surface became rougher than that exposed to ADT1 solution after 1992 h exposure (see Fig. 1(k) and (g)). However, no cracks occurred.

Optical micrographs (m)–(p) in Fig. 1 show the topographical changes of the sample's surface before and after exposure to ADT3 solution for 432 h, 1992 h and 3312 h, respectively. The surface became rough and some spot corrosion appeared after exposure for 432 h. The cracks initiated and propagated on the surface of the silicone rubber after exposure for 1992 h. The extent of surface damage in ADT3 solution is severer compared to other solutions (i.e. RS, ADT1 and ADT2 solutions) under identical conditions. From the optical microscopy results, it can be concluded that (a) the surface damage of the silicone rubber samples in highly concentrated solutions is severer, and (b) the degradation started from surface roughness and finally cracks, exhibiting time-dependent and acid-dependent process.

3.2. ATR-FTIR

ATR-FTIR was conducted on the silicone rubber samples before and after exposure to the test solutions to study the chemistry change. Fig. 2(A) and (B) shows the IR spectra ranging from

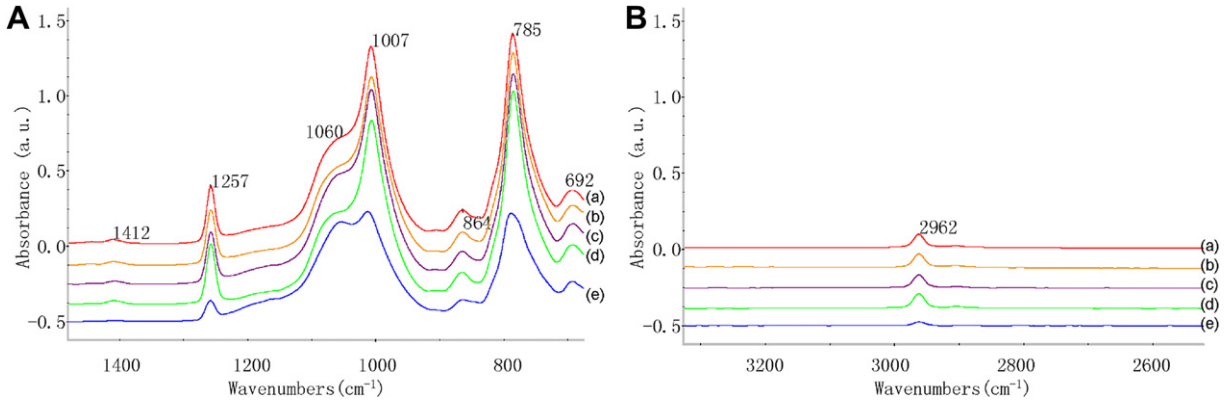

Fig. 2. ATR-FTIR test results (A: spectra from 690 to 1500 cm^{-1}, and B: from 2500 to 3300 cm^{-1}) for the sample exposed to test solutions at 70 °C: (a) without exposure, after (b) 432 h to RS, (c) 432 h to ADT1, (d) 432 h to ADT2, (e) 432 h to ADT3.

690 cm^{-1} to 1500 cm^{-1} and from 2500 cm^{-1} to 3300 cm^{-1} for the samples after 432 h exposure, respectively. Fig. 3(A) and (B) shows the IR spectra ranging from 690 cm^{-1} to 1500 cm^{-1} and from 2500 cm^{-1} to 3300 cm^{-1} for the samples after 1992 h exposure, respectively. The spectra a, b, c, d and e in Figs. 2 and 3 represent the samples before and after exposure to RS, ADT1, ADT2 and ADT3 solutions, respectively.

The strongest and broadest peaks for the unexposed samples (see Figs. 2(a) and 3(a)) are between 1007 cm^{-1} and 1060 cm^{-1}, and there are other peaks at 785 cm^{-1}, 1257 cm^{-1}, 864 cm^{-1}, 692 cm^{-1}, 1412 cm^{-1} and 2962 cm^{-1}. The peaks at 1007 cm^{-1} to 1060 cm^{-1} are from the stretching vibrations of Si—O—Si present in the silicone rubber backbone. The peak at 785 cm^{-1} is due to the vibrational coupling between the Si—C stretching vibration mode and the CH_3 rocking vibration mode for the Si—CH_3 group. The peaks at 1257 cm^{-1} and 864 cm^{-1} are due to the bending vibration of Si—CH_3 and the rocking vibration of Si—CH_3, respectively. The peak near 1412 cm^{-1} is due to the rocking vibration of —CH_2— as a part of the silicone rubber crosslinked domain. The peaks at 692 cm^{-1} and 2962 cm^{-1} are due to the stretching vibration of CH_3. The correspondence between the wavenumber and the vibration mode is referred [25].

For silicone rubber samples exposed to the regular solution up to 432 h and 1992 h (see Figs. 2(b) and 3(b)), the intensity of the peaks at 1007 cm^{-1} to 1060 cm^{-1} did not change significantly compared to that of the unexposed samples (see Figs. 2(a) and 3(a)). The intensity of the other peaks had no obvious changes. This result denotes that the surface chemistry on the surfaces of silicone rubber samples did not change apparently in regular solution. This result is consistent with that observed by optical microscope.

For silicone rubber samples exposed to ADT1 solution up to 432 h (see Fig. 2(c)) and up to 1992 h (see Fig. 3(c)), the intensity of the peaks between 1007 cm^{-1} and 1060 cm^{-1} decreased slightly.

For silicone rubber samples exposed to ADT2 solution up to 432 h (see Fig. 2(d)) and up to 1992 h (see Fig. 3(d)), the intensity of the peaks between 1007 cm^{-1} and 1060 cm^{-1} decreased more sharply than that of the samples mentioned above. The intensity of the other peaks did not change obviously.

For silicone rubber samples exposed to ADT3 solution up to 432 h and 1992 h (see Figs. 2(e) and 3(e)), the intensity of the peaks between 1007 cm^{-1} and 1060 cm^{-1}, 785 cm^{-1}, 1257 cm^{-1}, 864 cm^{-1} and 2962 cm^{-1} decreased dramatically after 432 h and 1992 h exposure, respectively. And also, the intensity of the peak at 692 cm^{-1} decreased over time. The peaks at 1257 cm^{-1} and at 2962 cm^{-1} almost disappeared after 1992 h exposure. The peak at 1412 cm^{-1} disappeared after 1992 h exposure.

From Figs. 2 and 3, it can be seen that for samples exposed to RS, ADT1 and ADT2 solutions, the intensity of the peaks from 1007 cm^{-1} to 1060 cm^{-1} decreased, but there is no obvious changes occurred at other peaks (i.e. 785 cm^{-1}, 1257 cm^{-1}, 864 cm^{-1}, 692 cm^{-1}, 1412 cm^{-1} and 2962 cm^{-1}). This could be due to the damage of the Si—O—Si (spectra from 1007 cm^{-1} to 1060 cm^{-1}) in the backbone of silicone rubber by the acid. For samples in ADT3 solution, the intensity of all peaks had large changes. This could be due to the high concentration of acidic solution. The higher the concentration of the acid in solutions, the more the material

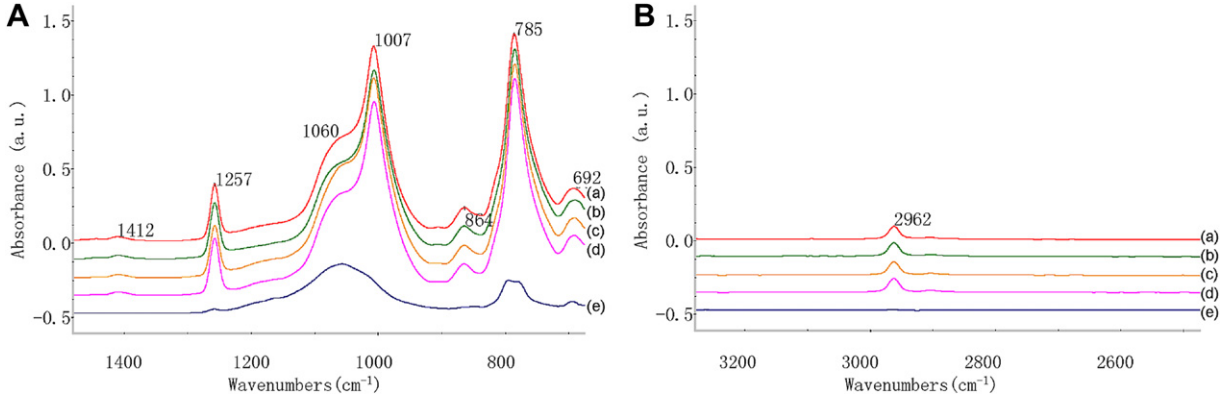

Fig. 3. ATR-FTIR test results (A: spectra from 690 to 1500 cm^{-1} and, B: from 2500 to 3300 cm^{-1}) for the sample exposed to test solutions at 70 °C: (a) without exposure, after (b) 1992 h to RS, (c) 1992 h to ADT1, (d) 1992 h to ADT2, (e) 1992 h to ADT3.

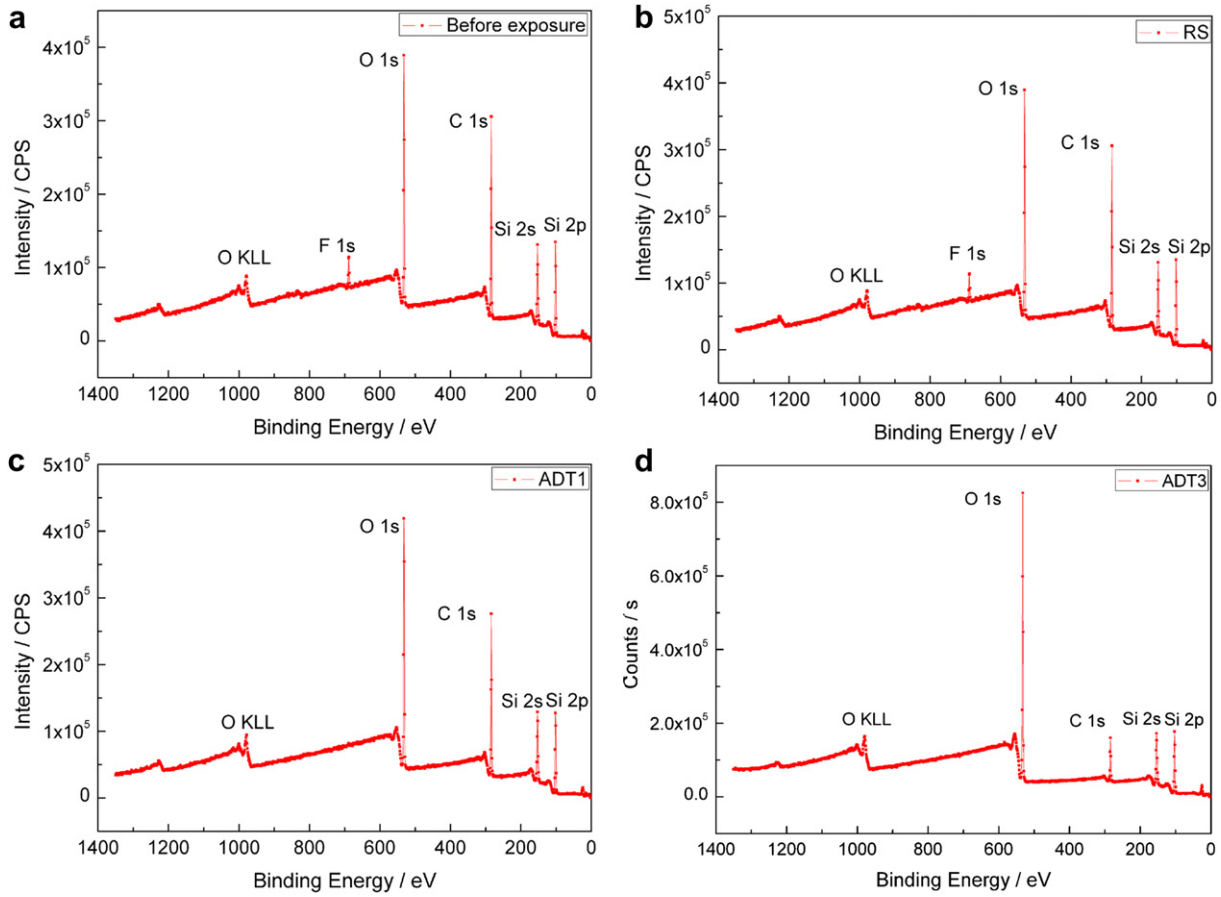

Fig. 4. XPS survey spectra for silicone rubber samples before and after exposure to test solutions at 70 °C: (a) before exposure, (b) 1992 h exposure to RS, (c) 1992 h exposure to ADT1 (d) 1992 h exposure to ADT3.

degraded. The results reveal that the degradation and degradation mechanisms are similar for the samples exposed to the different test solutions.

From ATR-FTIR results, it can be obtained that the chemical degradation is probably due to the hydrolysis of crosslink sites and chain scissoring in the silicone rubber backbone under such conditions. The chemical changes in the silicone rubber backbone could be due to the attack of the Si–O–Si by strong acid, especially Fluoric acid, to form Si–OH. And then the Si–OH could be converted to Si–O. This caused significant chemical changes [19,26–28].

3.3. X-ray photoelectron spectroscopy

In order to study the degradation mechanisms of silicone rubber exposed to PEM fuel cell environment, XPS analysis was conducted.

Table 1
Surface atomic concentration of each element and ratios of atomic concentrations of O and C to Si for silicone rubber samples before and after exposure to test solutions at 70 °C.

Samples	Atomic concentration (at.%)				Ratios to Si	
	C	O	Si	F	C/Si	O/Si
Before exposure	46.13	25.49	27.74	0.64	1.663	0.919
1992 h exposure in RS	44.01	27.10	28.28	0.6	1.556	0.958
1992 h exposure in ADT1	43.66	27.08	28.98	0.28	1.507	0.934
1992 h exposure in ADT3	21.08	45.94	32.81	0.17	0.642	1.400

Fig. 4(a)–(d) shows XPS survey spectra for the samples before and after 1992 h exposure to regular solution, ADT1 and ADT3 solutions at 70 °C, respectively.

The spectra (see Fig. 4(a)–(d)) revealed the presence of carbon (C), oxygen (O), silicon (Si) and small amount of fluorine (F). The atomic concentrations of these elements are given in Table 1. From Fig. 4, it can be seen that the carbon peak decreased and the oxygen peak increased with exposure time and acid content. Especially, the carbon peak and oxygen peak changed significantly for samples

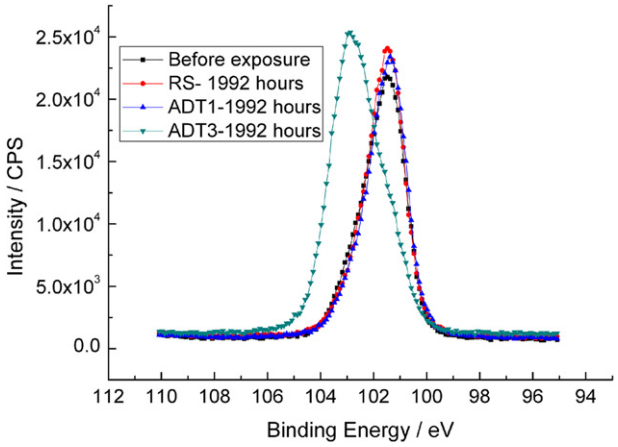

Fig. 5. Si2p high resolution spectra for the samples at different test conditions.

exposed to ADT3 solution. Table 1 also gives the ratios of concentration (C/Si and O/Si) for samples before and after exposure over time. As shown in Table 1, the C/Si ratio decreased dramatically with increasing exposure time and acid concentration. This could be due to that the methyl group on the silicon atom was attacked and oxidized to form the Si–O bonds. The increase of O/Si ratio with exposure time may indicate that the chain in the backbone (–Si–O–Si–) was attacked and broken.

In order to study the degradation mechanisms for the sample exposed to the test environments further, the high-resolution XPS analysis was also conducted. The Si2p high resolution spectra of silicone rubber before exposure and after exposure to RS, ADT1 and ADT3 solutions for 1992 h are shown in Fig. 5. The O1s high resolution spectra of silicone rubber before exposure and after exposure to RS, ADT1 and ADT3 solutions for 1992 h are shown in Fig. 6. From Figs. 5 and 6, it can be seen that the binding energies for silicone rubber sample exposed to RS and ADT1 solution had no obvious changes. For the silicone rubber sample exposed to ADT3 solution for 1992 h, the Si2p shifted 2 eV (see Fig. 5) to higher binding energy level and the O1s had a shift 1 eV (see Fig. 6) toward higher binding energy. This result indicates that the main chain in the silicone rubber backbone (–Si–O–Si–) damaged to form Si–O.

In order to obtain more detailed information about the chemical changes for the samples exposed to the simulated PEM fuel cell environments, curve fitting was used to deconvolute both unexposed and exposed samples for Si2p and O1s regions. The high resolution XPS results from the curve fitting of Si2p and O1s spectra for the samples before and after 1992 h exposure are shown in Figs. 7 and 8, respectively.

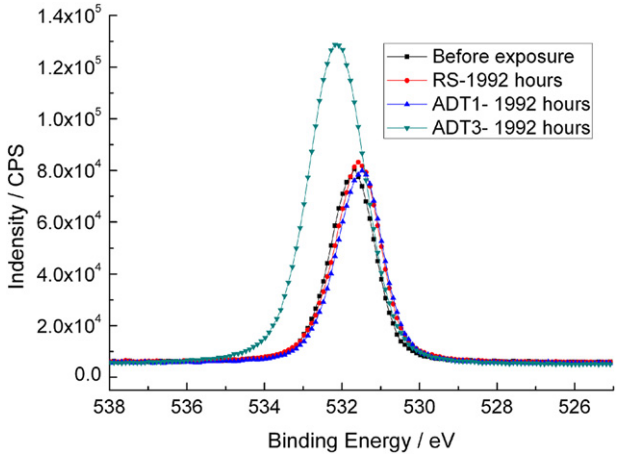

Fig. 6. O1s high resolution spectra for the samples at different test conditions.

The fitted results of Si2p spectrum for samples before exposure and after exposure to RS, ADT1 and ADT3 solutions are shown in Fig. 7(a)–(d), respectively. The Si2p spectrum in Fig. 7(a) could be fitted to two components corresponding to two peaks at the binding energies of 102 eV and 101.3 eV. The first peak at the binding energy of 102 eV is assigned to Si–O–Si [29] bonds and is related to the backbone of the silicone rubber. The second peak at the binding energy of 101.3 eV is related to the $Si–CH_3$ [29] in the silicone rubber present as the side group. When the silicone rubber

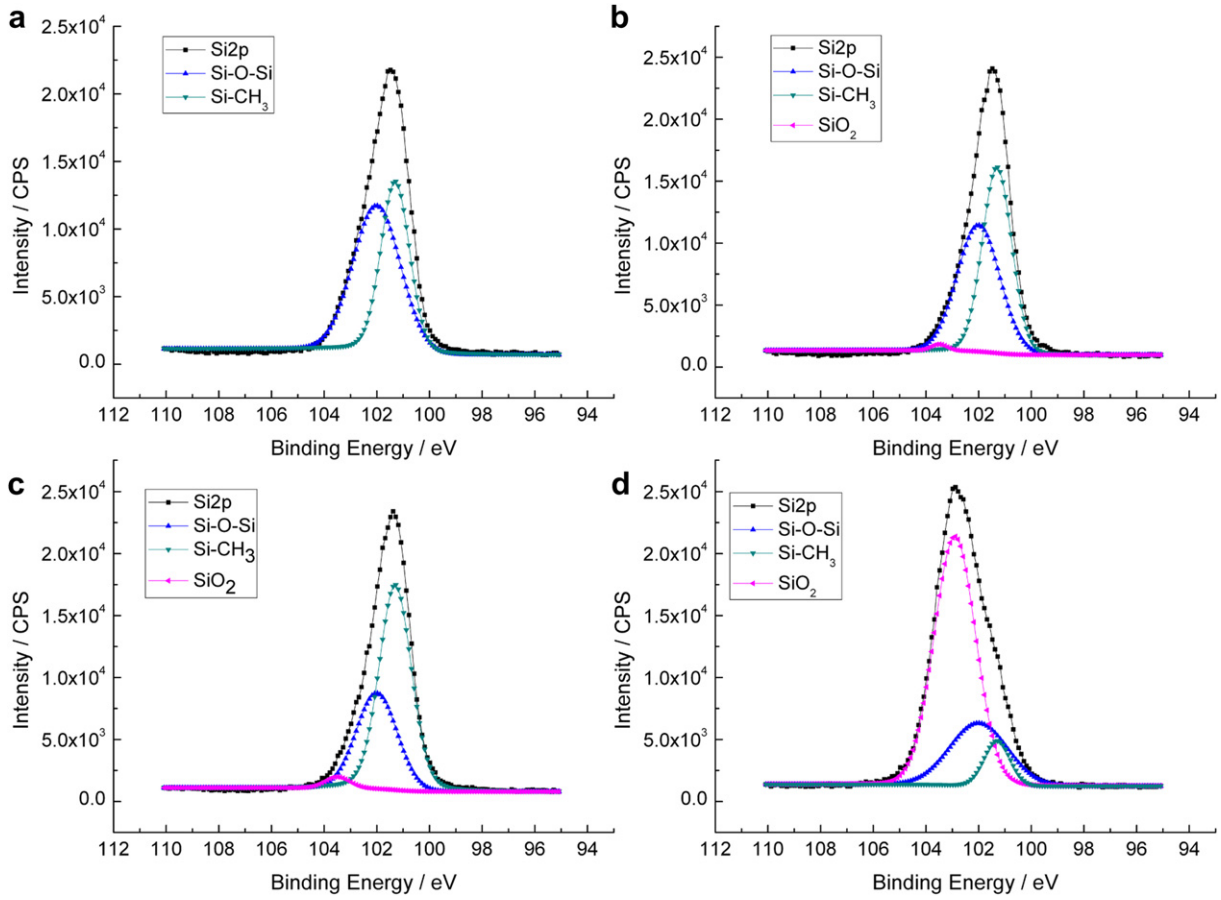

Fig. 7. Si2p high resolution spectra for the sample before exposure and after exposure to test solutions for 1992 h: (a) Si2p-before exposure, (b) Si2p-RS, (c) Si2p-ADT1, (d) Si2p-ADT3.

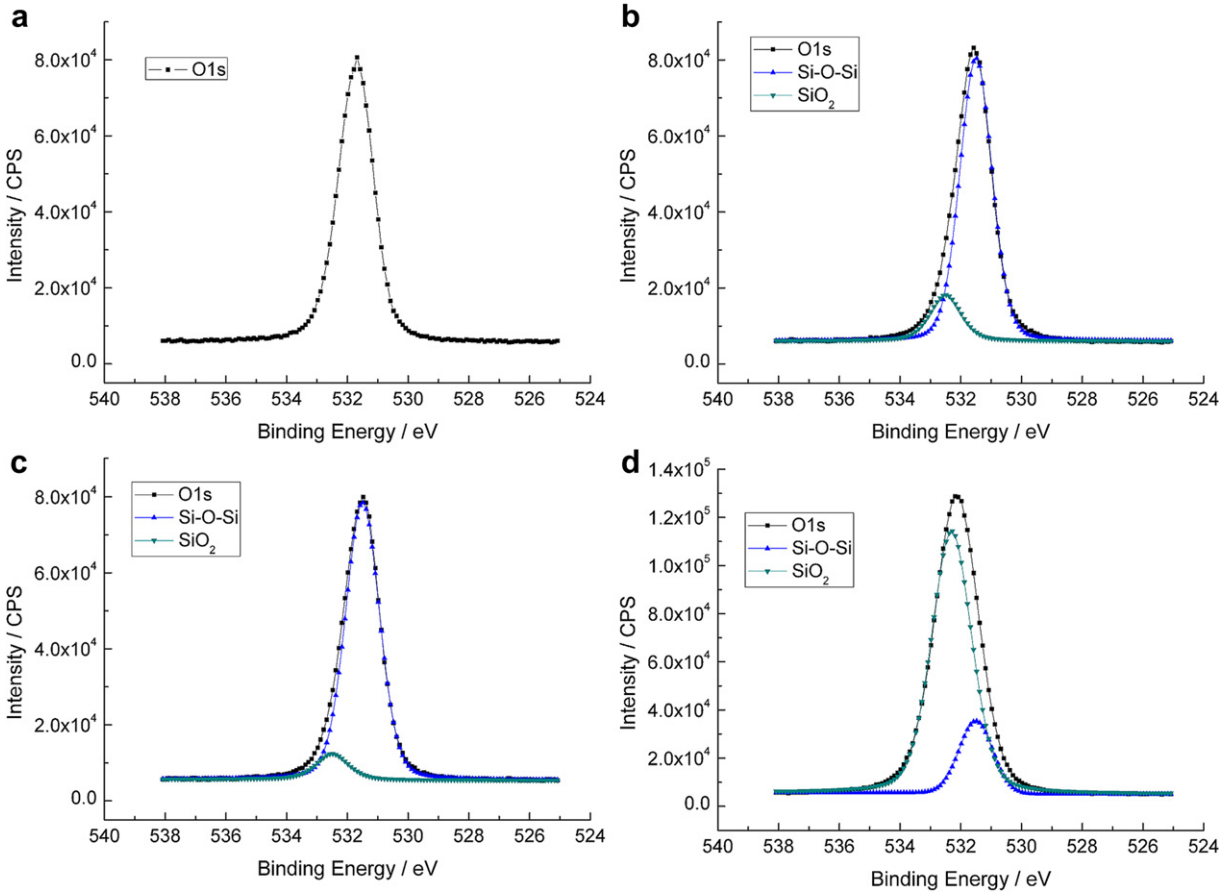

Fig. 8. O1s high resolution spectra for the sample before exposure and after exposure to test solutions for 1992 h: (a) O1s-before exposure, (b) O1s-RS, (c) O1s-ADT1, (d) O1s-ADT3.

was exposed to regular solution for 1992 h, the Si2p XPS spectrum in Fig. 7(b) could be fitted to three components corresponding to three peaks at the binding energies of 102 eV, 101.3 eV and 103.5 eV. The additional peak of 103.5 eV (Fig. 7(b) vs Fig. 7(a)) is assigned to SiO_2 [29], which is a new component appeared in the process of degradation of silicone rubber. When the silicone rubber was exposed to ADT1 solution for 1992 h, the Si2p XPS results from the curve fitting of the Si2p spectrum (see Fig. 7(c)) are similar to that for the samples exposed to the regular solution at the same exposed time. In Fig. 7(c), the intensity of peak at 102 eV (Si—O—Si) decreased and the intensity of peak at 103.5 eV (SiO_2) increased. After the silicone rubber was exposed to ADT3 solution for 1992 h, the Si2p XPS spectrum in Fig. 7(d) could be fitted to the three components corresponding to the three peaks at the same binding energies of 102 eV, 101.3 eV and 103.5 eV. However, the intensity of peaks at binding energies of 102 eV (Si—O—Si) and 101.3 eV ($Si—CH_3$) decreased significantly. In the mean time, the intensity of peak at binding energy of 103.5 eV (Si—O) increased dramatically. This result demonstrates further that the backbone of silicone rubber is destroyed and the silicone rubber degrades. The degradation mechanisms are similar for the silicone rubber exposed to the different test solutions studied at this work.

The fitted results of O1s XPS spectrum for samples before and after exposure to RS, ADT1 and ADT3 solutions are shown in Fig. 8(a)–(d), respectively. The O1s spectrum in Fig. 8(a) could be fitted by one single peak at the binding energy of 531.5 eV. This peak corresponds to Si—O—Si [29] bonds in the backbone of the silicone rubber. When the silicone rubber was exposed to regular solution for 1992 h, the O1s XPS spectrum as displayed in Fig. 8(b), could be fitted by two dominant peaks at the binding energies of 531.5 eV and 532.5 eV. The additional peak of 532.5 eV is assigned to SiO_2 [29], which is a new composition appeared in the process of degradation of silicone rubber. When the silicone rubber was exposed to ADT1 solution for 1992 h, the O1s XPS results from the curve fitting of the O1s spectrum (see Fig. 8(c)) are similar to that for the samples exposed to the regular solution at the same exposed time. When the silicone rubber was exposed to ADT3 solution, it can be seen that the intensity of peak at binding energy 531.5 eV decreased sharply. Meanwhile, the intensity of peak at binding energy 532.5 eV increased dramatically. This result indicates that the silicone rubber degrades severely.

These changes of chemical structures reflect the chemical degradation of silicone rubber exposed to the test solutions. The chemical degradation proceeded via de-cross-linking and chain scission in the backbone accompanied with the damage of the fillers in the samples. The degradation may affect the mechanical properties of the silicone rubber as gaskets, the long-term durability and performance of PEM fuel cell. The XPS results are in agreement with the FTIR observations.

4. Conclusions

Degradation process and degradation mechanisms of the silicone rubber, a commercial available elastomeric gasket material, were investigated in one simulated PEM fuel cell environment and three ADT solutions. The following conclusions can be obtained:

(1) Optical microscopy indicates that surface topography of the sample exhibited time-dependent and acid-dependent degradation, and the degradation started from surface roughness

and finally resulted in cracks for the samples after exposure to test environments.

(2) ATR-FTIR spectrometry and XPS results reveal that the surface chemistry changed significantly as an indication of the chemical degradation of the silicone rubber material exposed to the test environments. The degradation mechanisms could proceed via de-crosslinking through hydrolysis of crosslink sites and chain scissoring in the backbone. The degradation mechanisms are similar for the silicone rubber exposed to the test solutions studied at this work.

(3) Current work is to show the chemical degradation and degradation mechanisms on the silicone rubber material in a simulated and three accelerated PEM fuel cell environments. The chemical degradation may cause the mechanical property changes. Studies on the degradation in mechanical properties of the silicone rubber after exposure to the environments are under investigation and will be reported later. It is expected that an appropriate method will be found to investigate the life time of the gaskets in PEM fuel cell environment.

Acknowledgments

The work is sponsored by the Natural Science Foundation of China (51175241), the Natural Science Foundation of Jiangsu Province in China (BK2009362), the innovation Program for Graduate Students in Nanjing University of Technology (BSCX200904) and the Innovation Project for College Graduates of Jiangsu Province in China (CXZZ11_0335). The assistance from Professor Y.J. Chao of University of South Carolina is acknowledged.

References

[1] J. Tan, Y.J. Chao, M. Yang, W.K. Lee, J.W. Van Zee, Int. J. Hydrogen Energy 36 (2011) 1846–1852.
[2] Y. Akiyama, H. Sodaye, Y. Shibahara, Y. Honda, S. Tagawa, S. Nishijima, J. Power Sources 195 (2010) 5915–5921.
[3] G. Liu, H. Liu, Y. Liu, S. He, Polym. Degrad. Stab. 96 (2011) 732–738.
[4] B.H. Youn, C.S. Huh, IEEE Trans. Dielect. Electr. Insul. 12 (5) (2005) 1015–1024.
[5] P.Y. Le Gac, V. Le Saux, M. Paris, Y. Marco, Polym. Degrad. Stab. 97 (3) (2012) 288–296.
[6] D. Graiver, K.W. Farminer, R. Narayan, J. Polym. Environ. 11 (4) (2003) 129–136.
[7] S. Mitra, A. Ghanbari-Siahkali, P. Kingshott, K. Almdal, H.K. Rehmeier, A.G. Christensen, Polym. Degrad. Stab. 83 (2004) 195–206.
[8] S. Mitra, A. Ghanbari-Siahkali, P. Kingshott, H.K. Rehmeier, H. Abildgaard, Kristoffer, Polym. Degrad. Stab. 91 (2006) 69–80.
[9] S. Mitra, A. Ghanbari-Siahkali, P. Kingshott, H.K. Rehmeier, H. Abildgaard, Kristoffer, Polym. Degrad. Stab. 91 (2006) 81–93.
[10] S. Miwa, T. Kikuchi, Y. Ohtake, K. Tanaka, Polym. Degrad. Stab. 96 (2011) 1503–1507.
[11] L. Ghassemzadeh, K.D. Kreuer, J. Maier, K. Müller, J. Power Sources 196 (2011) 2490–2497.
[12] Y.T. Hsu, K.S. Chang-Liao, T.K. Wang, C.T. Kuo, Polym. Degrad. Stab. 91 (10) (2006) 2357–2364.
[13] Y. Wang, L. Liu, Y. Luo, D. Jia, Polym. Degrad. Stab. 94 (2009) 443–449.
[14] Y. Chen, K. Hou, C. Lin, C. Bai, N. Pu, M. Ger, J. Power Sources 197 (2012) 161–167.
[15] C. Lin, C. Chien, J. Tan, Y.J. Chao, J.W. Van Zee, J. Power Sources 196 (2011) 1955–1966.
[16] J. Tan, Y.J. Chao, H. Wang, J. Gong, J.W. Van Zee, Polym. Degrad. Stab. 94 (2009) 2072–2078.
[17] J. Tan, Y.J. Chao, J.W. Van Zee, W.K. Lee, Mater. Sci. Eng. A 496 (2008) 464–470.
[18] J. Tan, Y.J. Chao, M. Yang, C.T. Williams, J.W. Van Zee, J. Mater. Eng. Perform. 17 (2008) 785–792.
[19] J. Tan, Y.J. Chao, X. Li, J.W. Van Zee, J. Power Sources 172 (2007) 782–789.
[20] J. Tan, Y.J. Chao, J.W. Van Zee, W.K. Lee, Mater. Sci. Eng. A 445-446 (2007) 669–675.
[21] Y. Wang, Ken S. Chen, Jeffrey Mishler, Sung Chan Cho, Xavier Cordobes Adroher, Appl. Energy 88 (2011) 981–1007.
[22] R. Borup, Jeremy Meyers, Bryan Pivovar, et al., Chem. Rev. 107 (10) (2007) 3904–3951.
[23] Guo Li, Jinzhu Tan, Jianming Gong, J. Power Sources 205 (2012) 244–251.
[24] Feng-Yuan Zhang, Suresh G. Advani, Ajay K. Prasad, et al., Electrochim. Acta 54 (16) (2009) 4025–4030.
[25] D. Lin-Vien, N.B. Colthup, W.G. Fateley, J.G. Grasselli, The Handbook of Infrared and Raman Characteristic Frequencies of Organic Molecules, Academic Press, Boston, 1991.
[26] W. Noll, Chemistry and Technology of Silicone, Academic Press, Boston, 1968.
[27] N. Yoshimura, S. Kumagai, S. Nishimura, IEEE Trans. Dielect. Electr. Insul. 6 (5) (1999) 632–650.
[28] F. Delor-Jestin, N.S. Tomer, R.P. Singh, J. Lacoste, E-Polymer 5 (2006) 1–13.
[29] J.F. Moulder, W.F. Stickle, P.E. Sobol, et al., Handbook of X-ray Photoelectron Spectroscopy, Perkin–Elmer Press, Minnesota, 1992.